Received: April 7, 2017 Revised: August 22, 2017 Accepted: August 25, 2017

(onlinelibrary.wiley.com) DOI: 10.1111/ner.12702

Avoiding Internal Capsule Stimulation With a New Eight-Channel Steering Deep Brain Stimulation Lead

Kees J. van Dijk, MSc *; Rens Verhagen, MSc †; Lo J. Bour, PhD†; Ciska Heida, PhD*; Peter H. Veltink, PhD*

Objective: Novel deep brain stimulation (DBS) lead designs are currently entering the market, which are hypothesized to provide a way to steer the stimulation field away from neural populations responsible for side effects and towards populations responsible for beneficial effects. The objective of this study is to assess the performances of a new eight channel steering-DBS lead and compare this with a conventional cylindrical contact (CC) lead.

Approach: The two leads were evaluated in a finite element electric field model combined with multicompartment neuron and axon models, representing the internal capsule (IC) fibers and subthalamic nucleus (STN) cells. We defined the optimal stimulation setting as the configuration that activated the highest percentage of STN cells, without activating any IC fibers. With this criterion, we compared monopolar stimulation using a single contact of the steering-DBS lead and CC lead, on three locations and four orientations of the lead. In addition, we performed a current steering test case by dividing the current over two contacts with the steering-DBS lead in its worst-case orientation.

Main Results: In most cases, the steering-DBS lead is able to stimulate a significantly higher percentage of STN cells compared to the CC lead using single contact stimulation or using a two contact current steering protocol when there is approximately a 1 mm displacement of the CC lead. The results also show that correct placement and orientation of the lead in the target remains an important aspect in achieving the optimal stimulation outcome.

Significance: Currently, clinical trials are set up in Europe with a similar design as the steering-DBS lead. Our results illustrate the importance of the orientation of the new steering-DBS lead in avoiding side effects induced by stimulation of IC fibers. Therefore, in clinical trials sufficient attention should be paid to implanting the steering DBS-lead in the most effective orientation.

Keywords: Computational modeling, deep brain stimulation, novel lead design, Parkinson's disease, steering-DBS

Conflict of Interest: The authors have no conflicts of interest to report.

INTRODUCTION

With FDA approval for almost 15 years, deep brain stimulation (DBS) of the subthalamic nucleus (STN) has become an established treatment for patients with Parkinson's disease (PD) (1,2). PD is a neurological movement disorder and the symptoms of the disease are closely related to pathological neural activity within the basal ganglia network (3). Because the STN is part of the basal ganglia network, STN-DBS directly modulates the pathological neural activity in the network by use of electric stimulation. Conventionally, this electric stimulation, a continuous train of electric pulses [typically with frequencies between 120 and 180 HZ, 1–5 mA amplitude, and 60–200 μsec pulse width (2)], is delivered in the STN through a lead containing four cylindrical contacts (CC) and is powered by a single source from a surgical implanted pulse generator. Until now the technology for DBS has not changed tremendously over the years (4,5). Lately however, technological developments have been reported in terms of new stimulation paradigms (6,7), closed-loop DBS (8–10), independent current source stimulators (11), and directional steering-DBS with high density and eight channel lead designs (12–14). Most of the new technologies are still in an early development phase, although some of the technologies are already used in clinic.

Steering-DBS is a method to overcome a big hurdle in DBS, that is, the stimulation of structures of fibers that cause side effects due to a small misplacement and/or displacement of the lead. The clinical outcome of the therapy is rather sensitive to the precise location of the lead with respect to the target (15,16). Unfortunately, displacement of 1–3 mm can occur during surgery or postsurgery due to several reasons, such as a postsurgery brain shift and inaccuracy of the stereotactic frame and limitations of imaging methods (17–20). In case of displacement of the lead, the stimulating electric field will influence the neurons and axons outside the intended

Address correspondence to: Kees J. van Dijk, MSc, University of Twente, Institute for Biomedical Engineering and Technical Medicine (MIRA), Biomedical Signals and Systems Group, Drienerlolaan 5, Zuidhorst 210 (Box 217), 7500 AE, Enschede, The Netherlands. Email: k.j.vandijk@utwente.nl

* MIRA Institute for Biomedical Engineering and Technical Medicine, University of Twente, Enschede, NL, The Netherlands; and

† Department of Neurology/Clinical Neurophysiology, Academic Medical Center, Amsterdam, NL, The Netherlands

For more information on author guidelines, an explanation of our peer review process, and conflict of interest informed consent policies, please go to http://www.wiley.com/WileyCDA/Section/id-301854.html

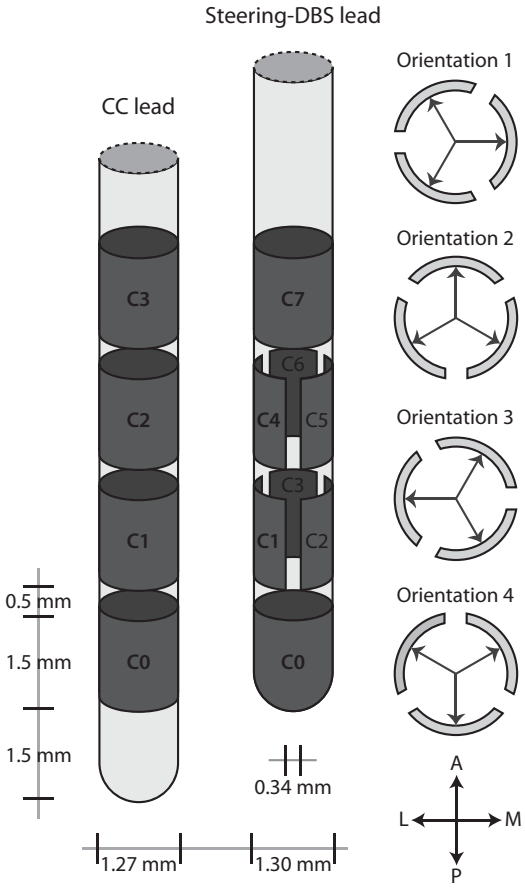

Figure 1. Representation of CC lead (left) and the Steering-DBS lead, with a schematic overview of the four orientations (right). Contact C1/C4 is pointing to medial (orientation 1), anterior (orientation 2), lateral (orientation 3), or posterior (orientation 4) direction.

target region. The target, the STN, is a small biconvex shaped structure surrounded by several bundles of myelinated axons such as the internal capsule (IC) (21). The large diameter, myelinated axons of the IC are easily stimulated which will induce unwanted side effects, such as dysarthria, muscle contractions, and gaze paresis (22).

To compensate for lead displacement, the stimulating electric field can be adjusted by selecting the appropriate electrode contact(s) on the lead. In this manner, with the conventional CC lead it is possible to compensate for a displacement along the direction of the lead. Eight channel lead designs, which started with a lead specifically designed for a study by Pollo et al. by Aleva Neurotherapeutics SA (Lausanne, CH) (14), followed by Boston Scientific (Marlborough, MA, USA) and St. Jude Medical (St. Paul, MN, USA), are also able to steer the electric field in the direction perpendicular to the lead. These leads have eight electrode contacts divided over four heights along the lead. For example, the lead by Boston Scientific contains a cylindrical shaped contact including the tip of the lead as the bottom electrode contact, followed by two cylinders which are split into three individual electrode contacts for directional steering-DBS, and the top electrode is a cylindrical shaped contact (Fig. 1). In addition, this eight-electrode contact lead design can be connected to a matching pulse generator with eight independent current courses. To assess the benefits of this particular steering-DBS system, clinical trials are currently set up in a number of clinics (23).

To aid clinicians in clinical trials, computational models can be used to give more insight in how steering-DBS is able to shape the electric field and affect the surrounding axons and neurons. Patient specific models which are used to visualize the potential field (24) and the volume of tissue activated (VTA), which is based on the spatial second order derivative of the potential field (25), can be a helpful tool for customized DBS-programming in patients. Multiple modeling studies have been performed to get a more accurate representation/estimation of the potential field and VTA by adding biological details in the model such as heterogeneous tissue conductivity, anisotropic conductivity, encapsulation layers, and tissue capacitive behavior (26–29). Next to the visualization, these more realistic models can also be used to automatically select stimulation parameters (30), to study new lead designs (12,14,31,32), and new stimulation paradigms such as coordinated reset (33). Previous studies on directional DBS electrodes have emphasized the potential improvement of the clinical effect by avoiding anatomical structures responsible for side effects (12,14). In a previous study by the authors, a high density (HD) directional DBS-lead containing 40 contacts, developed at Sapiens Steering Brain Stimulation BV, currently Medtronic Eindhoven Design center (Eindhoven, NL), was assessed in a computational model (34). Instead of looking at the potential field and VTA volume to avoid certain anatomical structures, this model included multicompartment neuron and axon models of two important neural populations in the subthalamic region, that is, the STN neurons, which represent the cells for positive clinical effect, and the IC fibers that will cause side effects when stimulated. Having the two neural populations in the model enabled adjustment of the contact configurations and stimulation amplitudes until the maximum number of activated STN cells was found without stimulating any of the axon fibers of the IC.

In this current study, we will use computational modelling procedures to assess the performance of a steering-DBS lead based on the eight-electrode contacts lead design. The model includes a heterogeneous anisotropic volume conductor model to compute the evoked potential field in the subthalmic region, and uses multicompartment neuron and axon models to investigate the stimulation effect of STN cells and the ability to avoid activation of IC fibers. We will compare this stimulation effect of the steering-DBS lead with the CC lead. The effect of one millimeter and 2-mm displacement is investigated, and as the new steering-DBS lead is not cylindrical symmetric we will also study the effect of four different orientations of the lead. Finally, we will test for this steering-DBS lead on each location and orientation the performance of monopolar stimulation vs. a current steering stimulation paradigm using two adjacent electrode contacts.

MATERIALS AND METHODS

The Computational Model

The model system of the DBS target region, the implanted DBS lead, and the stimulation effect on nearby neurons and axons, is based on previous work by Chaturvedi et al. (26,35). The model system consists of two consecutive parts. In the first part, the static electric field generated by current controlled stimulation (36), was computed in a finite element method (FEM) model of an adult brain. The geometry and conductivity of the brain is based on a human brain atlas consisting of a T1 MRI and a diffusion tensor imaging (DTI) dataset, with dimensions of 178 mm by 159 mm by 120 mm (37). The DTI dataset was used to estimate the anisotropy and heterogeneity of the tissue conductivity. A linear transformation (0.8 S/mm^2 scaling factor) was used to convert the diffusions tensors into conductivity tensors (38). The FEM model contains the DBS lead

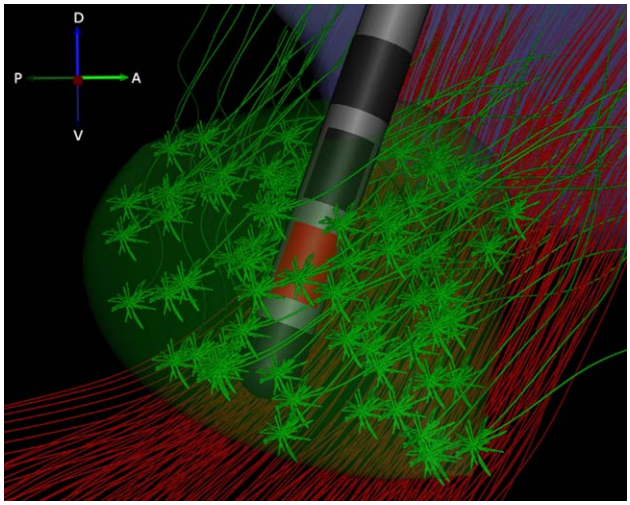

Figure 2. The visualization of the anatomical model of the subthalamic region with the steering-DBS lead at the center of the STN. Two relevant nuclei are shown: the STN (green volume in center), and the globus pallidus (purple volume in the background). The green STN cells originate from the STN volume and project to the globus pallidus. The red IC fibers are passing by underneath the STN. D, dorsal; V, ventral; P, posterior; A, anterior. [Color figure can be viewed at wileyonlinelibrary.com]

with a 0.5 mm tissue encapsulation layer (0.18 S/m) around the lead to account for the chronic electrode impedance of around 1 kΩ for the CC lead (mean impedance of 1005 Ω ± 6.8 Ω standard deviation for the CC lead contacts in the model). The complete geometry was divided into 4.1 million tetrahedral elements. The outer boundary was set to 0 V and Dirichlet boundary conditions were used. With this FEM model, the potential field generated by the stimulation was calculated by solving the Poisson equation in three-dimensions in SCIRun v3.0.2 (University of Utah, Salt Lake City, USA).

In the second part, the effect of the electric field on nearby cells was computed in a multicompartment neuron model programmed in NEURON 6.2 (Yale university, New Haven, USA) (39). Two neural populations are included in the model, that is, the STN projection cells and the IC fibers. The anatomical geometry of the IC fibers were defined through streamline tractography within SCIRun using the DTI dataset. With this, 200 fibers were tract from a seedbox (5 by 1 by 2 mm) located ventral-lateral to the STN. Three types of STN cells were placed in the model, each type projecting to the globus pallidus with a slightly different axon trajectory (35,40). The somas of the STN cells were placed randomly within the atlas-defined border of the STN volume. Every axon is implemented with the same model parameters [5.7 μm axon diameter model (41)]. This cable model includes detailed representations of the nodes of Ranvier, paranodal, and intermodal sections of the axons. For visualization purposes, the output from the second part of the model system was again imported in SCIRun v3.0.2 (Fig. 2).

DBS Lead Geometry

Either a CC lead or a steering-DBS lead (Fig. 1) was incorporated within the FEM model. The CC lead was based on the Medtronic 3389 electrode (Medtronic Inc., Minneapolis, US), which has a body diameter of 1.27 mm and carries four cylindrical contacts (C0-C3). These contacts each have a length of 1.5 mm, a 6 mm^2 contact surface area, and an interelectrode spacing of 0.5 mm. The steering-DBS lead was based on the design now commercially available by Boston Scientific (Marlborough, MA, USA), which has a body diameter of 1.3 mm and carries eight contacts (C0–C7). C0 is the contact at the tip of the lead with a length of 1.5 mm and 6 mm^2 contact surface area. Contacts C1–C6 form two rings, each of three steering-DBS contacts with a length of 1.5 mm and 1.6 mm^2 contact surface area. Contact C7 has the same shape as a standard CC lead contact. The interelectrode spacing along the lead is 0.5 mm and the interelectrode circumferential spacing between the steering-DBS electrode contacts (C1–C6) is 0.34 mm.

DBS Lead Location and Orientation

Three locations of the lead were assessed in the model, that is, the center location, a 1 mm off-center location, and a 2 mm off-center location. For the center location, The CC lead lies inside the STN with the center of contact C1 at the centroid of the STN. In case of the steering-DBS lead the combined center of C1–C3 was located at the centroid of the STN. For the 1 and 2 mm^2 off-center location the lead was shifted on a line between the centroid of the STN and the middle position of the nearest axon segments for each IC fiber in the model. This resulted in our datasets in a shift of 0.46, 0.59, and 0.66 mm in posterior, medial, and ventral directionally shift per 1 mm displacement. Unlike the CC lead, the steering-DBS lead is not fully symmetric with respect to the axis of the lead. Therefore, we included four different orientations of the six steering electrode contacts (Fig. 1). The trajectory of the lead was kept constant in all cases, whereas the lead approached the target in an AC/PC-based coordinate system with a typical lead arc and collar angle of 20° and 100°, respectively.

Stimulation Protocols

For the CC lead, each of the four electrode contacts were selected consecutively for stimulation with increasing stimulation amplitude up to a value at which IC fibers were activated. For the steering-DBS lead, we tested two types of stimulation protocols. First, a single contact stimulation protocol was used, where stimulation on each of the individual single contacts was simulated (Fig. 3) with increasing stimulation amplitudes up to a value at which IC fibers were activated. Second, a current steering stimulation protocol was used, where the current was simultaneously injected through two adjacent contacts with specified percentages (20/80%, 40/60%, 60/40%, 80/20%) of the total current divided over both contacts, again with increasing stimulation amplitudes up to a value at which IC fibers were activated.

The stimulation signal was a monopolar biphasic charge-balanced current pulse, that is, a 100 μsec rectangular waveform, with the total injected current ranging from −1 to −5 mA with a 0.5 mA step size, followed by a 5 msec period of low amplitude charge balanced anodic stimulation.

Activation of Neural Populations

The effect of the deep brain stimulation was evaluated in the neuron part of the computational model system: 15 datasets were created, five for each location of the lead. The STN cell bodies were randomly distributed inside the STN and the location of IC fibers was fixed. Each neuron or axon with a segment located at the position of the DBS lead was removed from the model. For the 15 datasets, this resulted in neuron models including 182.3 ± 13.1 IC fibers and 79.8 ± 4.3 STN cells. A cell or axon is counted as activated when the stimulation pulse evoked at least one action potential that propagated to the end segment of the axon.

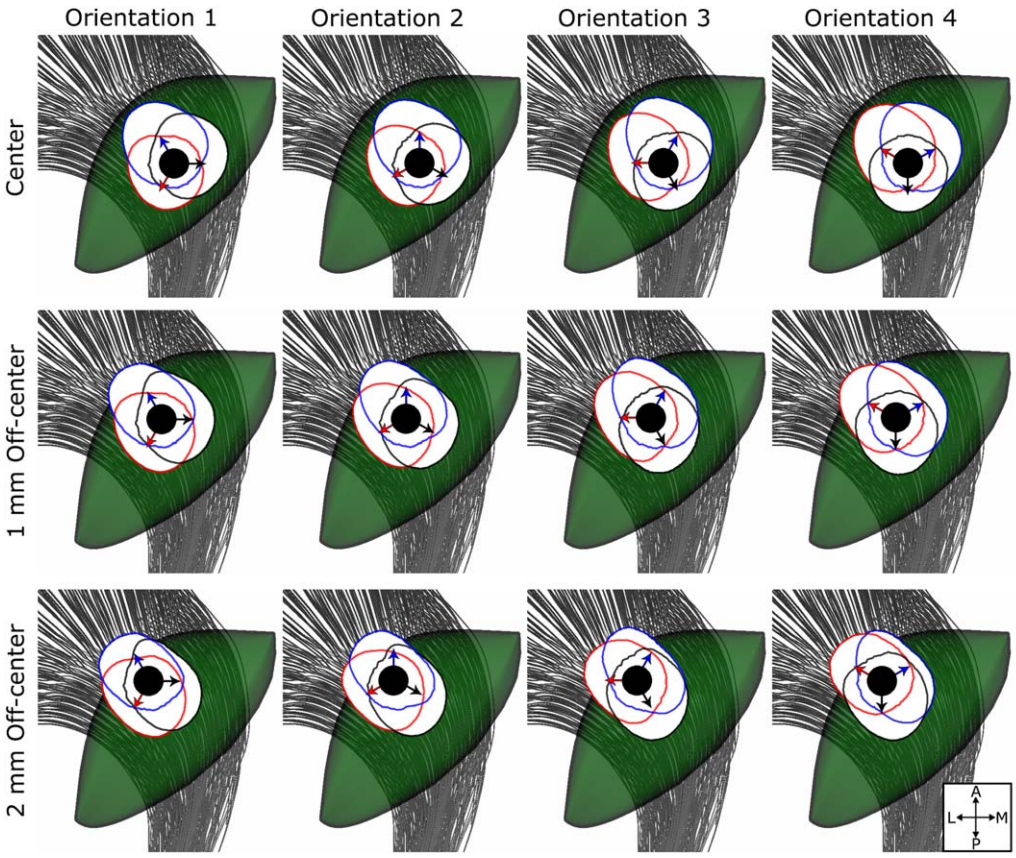

Figure 3. Top view of the STN (green volume) with the IC fibers running underneath the STN looking along the axis of the DBS-lead (black circle). On each of the lead locations and orientations, three iso-contours (0.1 V) of the potential field are shown in red, blue, and black, corresponding to monopolar stimulation (1 mA) through contact C4-C5-C6 heading in the direction of the color matched arrow. L, lateral; M, medial; P, posterior; A, anterior. [Color figure can be viewed at wileyonlinelibrary.com]

Statistical Analysis

To quantify the differences between stimulation protocols, we defined the optimal stimulation protocol as the configuration that activated the highest percentage of STN cells, without activating any of the IC fibers. A repeated measure ANOVA with significance level of 0.05 was performed, followed by a Bonferroni corrected multiple comparison procedure to statistically test the individual optimal stimulation effect in each situation. In each of the three lead locations, we compared each of the four lead orientations: optimal single contact stimulation vs. optimal current steering stimulation; optimal single contact stimulation vs. the optimal stimulation effect of the CC lead; finally, optimal current steering stimulation vs. the optimal stimulation effect of the CC lead.

RESULTS

We found for each lead location, orientation, and stimulation protocol the optimal stimulation settings. Figure 4 shows the percentage of STN cells which were activated and which denotes all significant differences between the different orientations (see Fig. 1 for the orientations) and the two stimulation protocols.

Single Contact Stimulation Protocol

At center location, the steering-DBS lead using single contact stimulation was able to activate 60.3 ± 4.8% STN cells in the first orientation, 75.1 ± 5.9% STN cells in the second orientation, 72.3 ± 3.9% STN cells in the third orientation, and 53.7 ± 2.5% STN cells in the fourth orientation. In the first orientation, the optimal stimulation was applied through the bottom medial contact (3 of 5 datasets) or the top posterior-lateral contact (2 of 5 datasets) with an amplitude of 4.1 ± 0.82 mA. In the fourth orientation, the optimal stimulation was through the bottom or top posterior contact with an amplitude of 4.3 ± 0.76 mA. In both the second and third orientation, the optimal stimulation was through the bottom posterior-medial contact with an amplitude of 5.0 ± 0.0 mA or 4.5 ± 0.0 mA, respectively.

At 1 mm off-center location, the steering-DBS lead was able to activate 35.8 ± 3.5% STN cells in the first orientation, 56.3 ± 5.4% STN cells in the second orientation, 59.8 ± 3.6% STN cells in the third orientation, and 44.3 ± 2.9% STN cells in the fourth orientation. The optimal stimulation settings used the top medial contact (2.0 ± 0.0 mA) and the top posterior contact (2.5 ± 0.0 mA) for the first and fourth orientation. In the second and third orientation, the optimal stimulation settings used the top posterior-medial contact (3.5 ± 0.0 mA and 4.0 ± 0.0 mA, respectively). Figure 5 shows the activated STN cells for the optimal stimulation setting in each of the four orientations.

At 2 mm off-center location, in each orientation, the steering-DBS lead was able to activate 6.4 ± 4.4% STN cells, while stimulating through the cylindrical contact C7 with an amplitude of 0.4 ± 0.22 mA.

Current Steering Stimulation Protocol

For most of the orientations and datasets, our current steering protocol prefers to steer the current into the posterior-medial

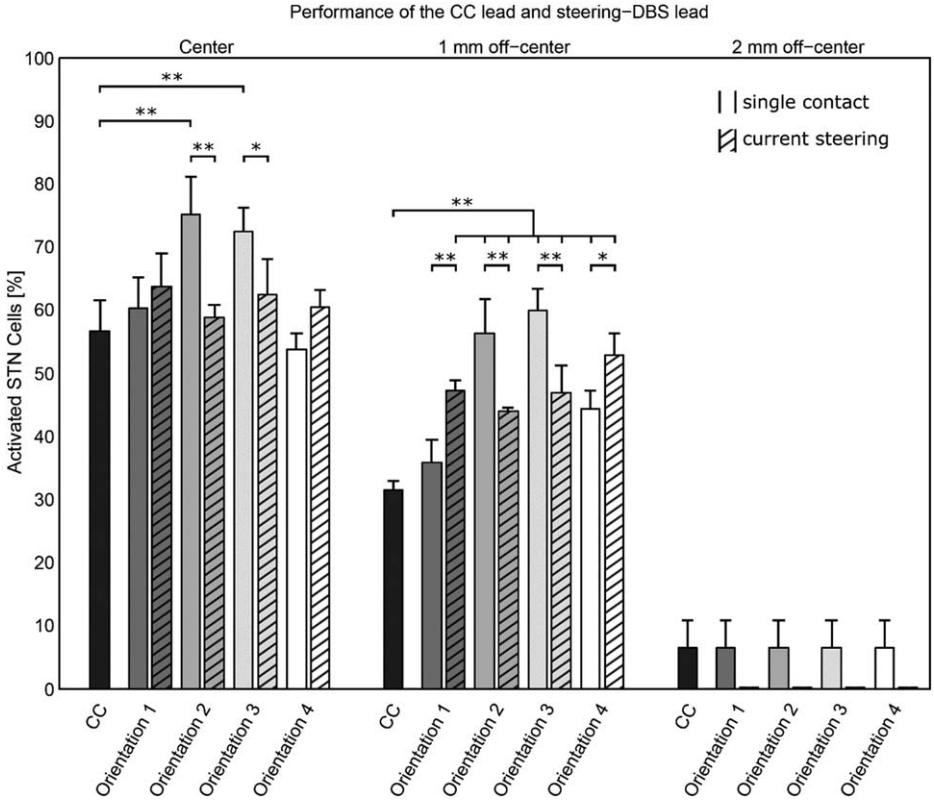

Figure 4. The performance of the five stimulation modes, that is, the CC and the four orientations of the steering-DBS lead. Bars denote mean values with standard deviations of the percentage of activated STN cells after stimulation for the 5 datasets per lead location each with random distributions of the STN cells. The nonhatched bars represent the results for single contact stimulation and the hatched bars represent the results for current steering stimulation. Significant differences are indicated with one asterisks ($p < 0.05$) or two asterisks ($p < 0.01$).

quadrant, only at the center location in the second orientation four datasets had the optimal stimulation toward the posterior-lateral direction, applying most of the total stimulation current in posterior direction.

At center location with the steering-DBS lead in its first orientation, it was able to activate 63.7 ± 5.2% STN cells by dividing the total current (3.8 ± 0.7 mA) over the medial contact and post-lateral contact (80/20% in four datasets and 60/40% in 1 dataset). In the second orientation, 58.7 ± 2.0% STN cells were activated by dividing the total current (4.4 ± 0.8 mA) over the postmedial and postlateral contact (80/20% in 1 dataset, 20/80% in 2 datasets, 40/60% in two datasets). In the third orientation, 62.5 ± 5.6% STN cells were activated by dividing the total current (3.80 ± 0.7 mA) over the postmedial and antero-medial contact (80/20% in 5 datasets). In the fourth orientation, 60.4%±2.9% STN cells were activated by dividing the total current (4.1 ± 1.0 mA) over the posterior and antero-medial contact (80/20% in 2 datasets and 60/40% in 3 datasets). Comparing the stimulation effect of our current steering stimulation protocol to single contact stimulation, we found a significant decrease of activated STN cells in the second orientation ($p < 0.01$) and in the third orientation ($p < 0.05$).

At 1 mm off-center location, the steering-DBS lead was able to activate 47.2 ± 1.5% STN cells in the first orientation by dividing the total current (2.5 ± 0.0 mA) over the medial contact and postlateral contact (80/20% in 2 datasets and 60%/40% in 3 dataset). In the second orientation, 43.9 ± 0.7% STN cells were activated by dividing the total current (2.5 ± 0.0 mA) over the postero-medial and postero-lateral contact (80/20% in 5 dataset). In the third orientation, 46.8 ± 4.4% STN cells were activated by dividing the total current (2.5 ± 0.0 mA) over the postero-medial and antero-medial contact (80/20% in 5 datasets). In the fourth orientation, 52.9 ± 3.4% STN cells were activated by dividing the total current (3.0 ± 0.0 mA) over the posterior and antero-medial contact (80/20% in 5 datasets). Comparing the stimulation effect of our current steering stimulation protocol to single contact stimulation, we found a significant decrease of activated STN cells in the second ($p < 0.01$) and third orientation ($p < 0.01$) and a significant increase in the first ($p < 0.01$) and fourth orientation ($p < 0.05$).

At 2 mm off-center location, the steering-DBS lead using the current steering protocol was not able to activate any STN cells without activating one or more IC fibers.

Comparison of the CC Lead and the Steering-DBS Lead

Finally, we statically compared the stimulation effect of the steering-DBS lead with the stimulation effect of the CC lead (Fig. 4). The CC lead, with its optimal stimulation settings, was able to activate 56.6 ± 4.8% STN cells at center location, 31.4 ± 1.4% of STN cells at 1 mm off-center location, and 6.4 ± 4.4% of STN cells at 2 mm off-center location (34). At center location, the steering-DBS lead using single contact stimulation was able to activate significantly more STN cells in the second and third orientation ($p < 0.01$). Interestingly, in none of the four orientations the steering-DBS lead using current steering stimulation was able to activate significantly more STN cells than the CC lead.

At 1 mm off-center location, a significant increase was found for all the orientations when using the current steering stimulation ($p < 0.01$), while using single contact stimulation a significant increase was found at the second, third, and fourth orientation

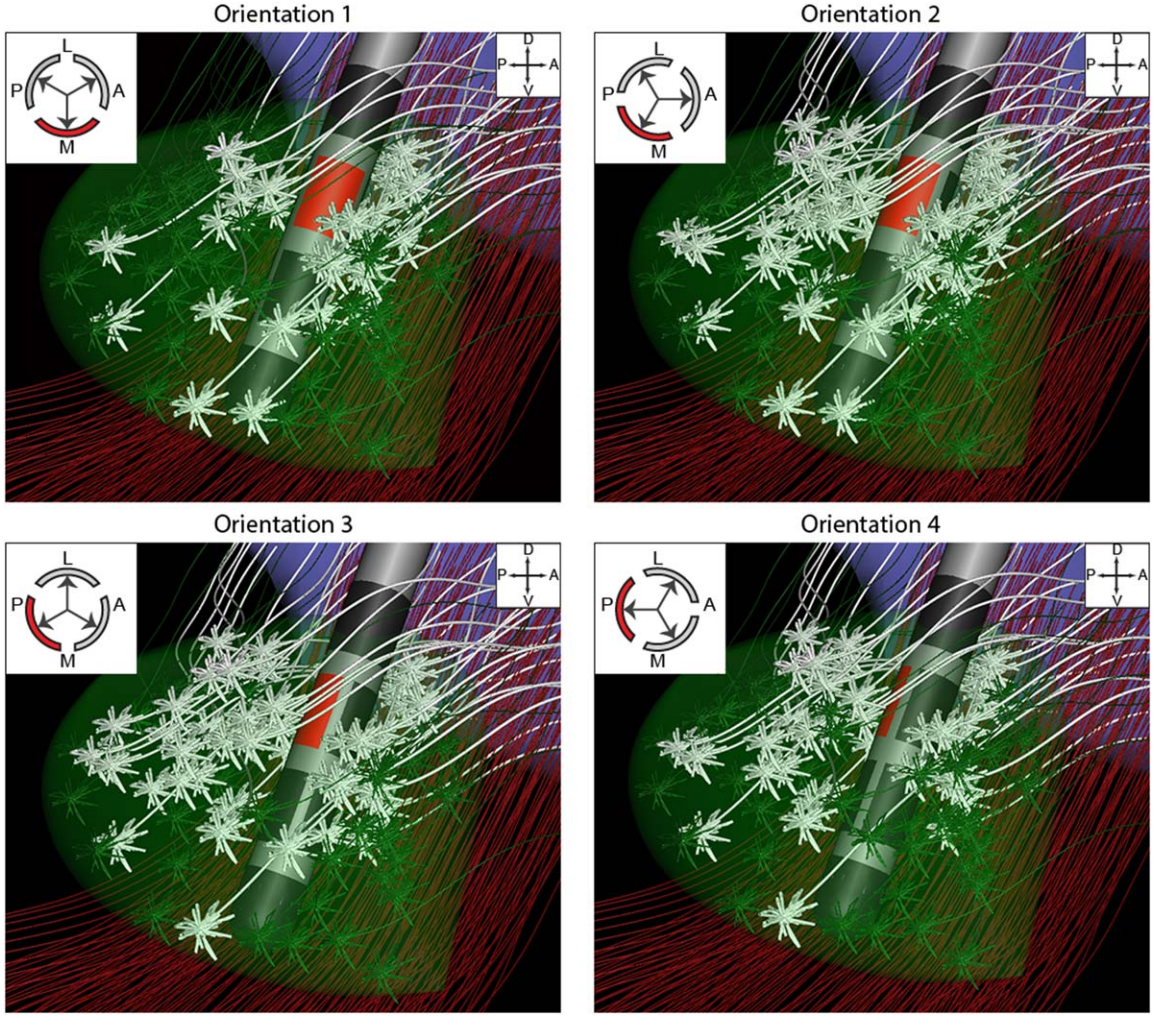

Figure 5. An example of the activation of STN cells illustrating the variability in the four orientations while using a monopolar stimulation protocol. The panels show a medial perspective of the STN (green volume), the globus pallidus (purple volume), IC fibers in red, and the STN cells in green and white. STN cells that were activated by the stimulation pulse are displayed in white. The stimulation pulse activated 35, 55, 61, and 49% of the STN cells in orientation 1–4, respectively. [Color figure can be viewed at wileyonlinelibrary.com]

($p < 0.01$). At 2 mm off-center location there were no significant differences found.

DISCUSSION

In this computational modeling study, we investigated a new steering-DBS lead design. The steering-DBS lead is able to shape the stimulation field by selecting appropriate electrode contacts for stimulation. In this manner, it is possible to stimulate target areas while not stimulating areas that cause side effects. Our results show that under the right circumstances, even using only single contact stimulation, the steering-DBS lead is indeed able to stimulate a significantly higher percentage of STN cells without activating any of the IC fibers compared to the CC lead. Especially in the case of a 1 mm displacement and the lead in optimal orientation, the steering-DBS lead outperforms the conventional lead. The current steering stimulation protocol shows that in case of a 1 mm displacement of the lead, where the single contact stimulation is performing weakly, dividing the stimulation current over two contacts opposing the IC can increase the percentage of activated STN cells. However, the results also show that correct placement and orientation of the lead within the target remains an important aspect for optimal stimulation outcome.

Using single contact stimulation at center and 1 mm off-center location, we found significantly different results in STN activation for the four orientations. The steering-DBS lead in its second and third orientation, which had an electrode contact in the opposite direction of the IC, the posterior-medial direction, was able to activate a significantly higher percentage of STN cells compared to the CC lead. The two other orientations did not have a steering electrode contact in opposite direction of the IC, which resulted in a less effective performance. Nevertheless, even in these two orientations the performances of the steering-DBS lead were never significantly worse than the CC lead and even at 1 mm off-center location the steering-DBS performed significantly better than the CC-lead while stimulating through the posterior contact (orientation 4).

The varied results that were obtained for the different orientations, illustrates a new challenge in correctly implanting the lead in the target. The lead contains a marker to verify the orientation of the lead by x-ray imaging. However, in order to make use of the full potential of the steering-DBS lead, the clinical effect of different orientations should be tested first during clinical trials. For this, computational models such as described in this study, can be a useful tool

to gain more insight in the effect of the different orientations and finding the correct orientation. Finally, future studies should assess besides lead displacements also the rotation of the lead over time, and find ways to guarantee a fixed orientation of the lead.

One way to compensate for the orientation dependency of the steering-DBS lead is current steering stimulation. We showed that by balancing current across the medial and posterior-lateral contact it is possible to increase the percentage of activated STN cells. This suggests that current steering enables stimulation in intermediate direction to a certain level. Unfortunately, stimulation through two contacts increases the active contact surface surrounding the lead, with which the selectivity of directional steering is reduced. This might explain why the current steering protocol is not performing better than stimulation through a cylindrical contact placed in the center of the STN. It should be noted that we presented the current steering separately from the single contact stimulation. In the clinic, the current steering protocol will be an addition to the single contact stimulation protocol. This means a clinician will not use the current steering protocol in case single contact stimulation is already the optimal stimulation protocol, such as in second and third orientation. Second, only current-steering through the two adjacent contacts on the same row was tested to show the potential of an easy to interpret current steering protocol. More advanced current steering patterns with multiple contacts might enable more selective stimulation, such that similar percentages of STN cells are activated as those achieved by using a single contact in posterior-medial direction. Third, it should be noted, more advantaged current steering patterns can also be performed with the CC lead. A previous modeling study, using similar methods, showed that the CC lead at the center of STN was able to activate 8% more STN cells using current steering with two independent sources than with monopolar stimulation (35). This will level out the performances of the leads, especially at center location. However, with a 1 mm displacement the decrease in performance of the CC lead is considerably larger than the decrease in performance of the directional lead. This indicates that the directional lead, within the 1 mm window, is less sensitive to the displacement away from the optimal center location.

At the 2-mm off-center location, we found no difference between de CC lead and the steering-DBS lead. This was due to the fact that the optimal electrode contact for both leads were the same top cylindrical contact, C3 and C7. The steering-DBS lead has only two rows of electrode contacts along the lead which can be used for steered stimulation (C1-C6). In the 2-mm displacement scenario, the two rows of steering electrode contacts were shifted 1.32 mm ventrally and ended up too close to the ventrally located axon segments of the IC fibers. This scenario illustrates that with the limited amount of rows of steering electrode contacts it remains important to position the lead at the correct depth. In addition, the possible advantage of this steering-DBS lead is vulnerable to a displacement along the trajectory of the lead.

We decided to include the model representation of the steering-DBS lead in a well-described model of the subthalamic region that included many important and realistic details. The technical limitations of this computational model are comprehensively described in previous studies, such as the large voxel size of the DTI dataset, and ignoring the capacitive behavior at the electrode-tissue interface (26,42,43). In this specific study, the large voxel size of the DTI dataset had an effect on two aspects of the model. First, the conductivity of the tissue in model was based on the DTI and this resulted in a low spatial resolution. Therefore, the anisotropy of small fiber bundles in the brain were not included in the model. Second, because of the low spatial resolution of the DTI dataset we were only able to trace the IC fibers and not the STN axons projecting to the pallidum. With respect to the capacitive behavior, in case of voltage controlled stimulation, the capacitive behavior of the electrode-tissue interface is important, especially for small contact surfaces area, because of its reduced electrode capacitance. However, while using current-controlled stimulation, similar to the one used in our current study, the electrode capacitance had negligible effects on the corresponding tissue voltage (28). A previous study on a segmented lead with similar contact surface areas as the one in our model also showed that including this capacitive behavior in their model did not significantly change their results (31). Finally, since our results focus on a comparison between the CC and HD leads in the same model, the limitations will influence both leads and therefore will have little impact on the comparison.

We should note that, in order to quantify the stimulation effect, we adopted the criterion that with DBS a maximum percentage of activated STN cells is needed while not stimulating the IC. Clinical research is needed to find more realistic and more detailed criterions. Therefore, our criterion should only be regarded as an example to show the steering effect on a plausible target while steering away from a region causing side effects. Using this criterion also meant we did not pay attention to power consumption. We believed maximizing the effect of DBS is of greater importance than battery lifetime, especially now that rechargeable implantable pulse generators have become available (44,45).

Because we used the same modelling procedure, we are able to compare the current results of the steering-DBS lead with a previously described 40 contact lead (34). This shows that at center and 1 mm off-center location the steering-DBS lead with the option to steer the stimulation field in posterior-medial direction performed very similar as the 40-contact lead. However, at 2-mm off-center location the HD lead was able to perform significantly better (10–11% more STN cells activated) than the CC lead, which was due to the fact that the dorsally located electrode contact of the 40-contact lead also can be used for steering. The previous study did not investigate different orientations of the 40-contact lead, however this lead is always able to stimulate in posterior-medial direction, and is, therefore, probably less sensitive to rotations of the lead.

Having only eight electrode contacts is a great advantage in programming the stimulation settings when monopolar stimulation is used. For a HD lead with a large number of electrode contacts programming the stimulation settings with a trial-and-error approach will not suffice in clinical practice (13). For a 32 HD lead, which was used in a proof of concept study the test stimulation was limited to four standard steering directions, because of time constraints (46). The eight-channel lead has the advantage that it can be combined with a novel internal pulse generator, which includes eight independent current sources (11). We used just a simple current steering stimulation protocol with two contacts, which already showed an improvement of the stimulation effect in certain cases. By selecting the appropriate current strength on each contact, the steering properties of DBS can be improved even more (35), however, finding the correct current for each of the eight contacts will highly increase the complexity of programming the stimulation parameters. Thus, unless new technological tools will be developed to aid clinicians in selecting the optimal stimulation settings, the theoretical advantage of having many contacts or many current sources might not be fully utilized in practice. Creating patient specific models, by using the patients MRI/DTI dataset and using the same methodology as the current study, can be one of these tools. Patient specific models effectively have been used before to select stimulation settings, which maximize neural activation in a certain area (30). Additionally, using the patient specific IC in the model can be used to warn the clinician to avoid certain settings.

Besides running through all possible settings in an electric field model, more advanced techniques based on machine learning (31) and particles swarm optimization (47) can be the next step in finding the optimal settings in a time efficient way.

CONCLUSION

In conclusion, we found that the concepts of steering the stimulation field with a steering-DBS lead with only eight channels may be beneficial compared to the conventional lead, and it allows to correct for lead displacement errors of approximately 1 mm when it has the correct orientation or using current steering. While using single contact stimulation, which has the advantage of being easy to use in the clinic, our results illustrate the importance of the orientation of this lead. Therefore, sufficient attention should be paid to implanting the steering DBS-lead in the most effective orientation, and to keep this orientation of the lead over time.

Acknowledgements

This work was supported by grants from Twente instituut voor neuromodulation (TWIN), Applied Scientific Institute for Neuromodulation. The authors would like to thank Ashutosh Chaturvedi and Cameron C. McIntyre for their help and providing the computational model of the subthalamic region.

Authorship Statements

Mr. Van Dijk and Mr. Verhagen worked on the model. Mr. Van Dijk did the data analysis and prepared the manuscript draft with important intellectual input from Drs. Bour, Heida, Veltink, and Mr. Verhagen. Mr. Verhagen and Dr. Bour gave advice in selecting the clinically relevant focus of the study. Drs. Veltink and Heida helped with the data analyses and statistical support. All authors had important input in drafting the paper and reviewing it critically. All authors approved the final manuscript.

How to Cite this Article:

van Dijk K.J., Verhagen R., Bour L.J., Heida C., Veltink P.H. 2017. Avoiding Internal Capsule Stimulation With a New Eight-Channel Steering Deep Brain Stimulation Lead. Neuromodulation 2017; E-pub ahead of print. DOI:10.1111/ner.12702

REFERENCES

1. Deuschl G, Schade-Brittinger C, Krack P et al. A randomized trial of deep-brain stimulation for Parkinson's disease. *N Engl J Med* 2006;355:896–908.
2. Breit S, Schulz JB, Benabid AL. Deep brain stimulation. *Cell Tissue Res* 2004;318:275–288.
3. Brown P. Oscillatory nature of human basal ganglia activity: relationship to the pathophysiology of Parkinson's disease. *Mov Disord* 2003;18:357–363.
4. Hariz M. Deep brain stimulation: new techniques. *Parkinsonism Relat Disord* 2014;20 (Suppl. 1):S192–S196.
5. Rossi PJ, Gunduz A, Judy J et al. Proceedings of the third annual deep brain stimulation think tank: a review of emerging issues and technologies. *Front Neurosci* 2016; 10:119.
6. Tass PA. A model of desynchronizing deep brain stimulation with a demand-controlled coordinated reset of neural subpopulations. *Biol Cybern* 2003;89:81–88.
7. Tass PA, Qin L, Hauptmann C et al. Coordinated reset has sustained aftereffects in Parkinsonian monkeys. *Ann Neurol* 2012;72:816–820.
8. Little S, Pogosyan A, Neal S et al. Adaptive deep brain stimulation in advanced Parkinson disease. *Ann Neurol* 2013;74:449–457.
9. Rossi L, Foffani G, Marceglia S, Priori A. Towards adaptive deep brain stimulation: recording local field potentials during stimulation. *Mov Disord* 2007;22:S234–S234.
10. Rosin B, Slovik M, Mitelman R et al. Closed-loop deep brain stimulation is superior in ameliorating Parkinsonism. *Neuron* 2011;72:370–384.
11. Timmermann L, Jain R, Chen L et al. Multiple-source current steering in subthalamic nucleus deep brain stimulation for Parkinson's disease (the VANTAGE study): a non-randomised, prospective, multicentre, open-label study. *Lancet Neurol* 2015;14:693–701.
12. Martens HC, Toader E, Decre MM et al. Spatial steering of deep brain stimulation volumes using a novel lead design. *Clin Neurophysiol* 2011;122:558–566.
13. Willsie AC, Dorval AD. Computational field shaping for deep brain stimulation with thousands of contacts in a novel electrode geometry. *Neuromodulation* 2015;18: 542–550. discussion 550–551.
14. Pollo C, Kaelin-Lang A, Oertel MF et al. Directional deep brain stimulation: an intraoperative double-blind pilot study. *Brain* 2014;137:2015–2026.
15. Hamel W, Fietzek U, Morsnowski A et al. Deep brain stimulation of the subthalamic nucleus in Parkinson's disease: evaluation of active electrode contacts. *J Neurol Neurosurg Psychiatry* 2003;74:1036–1046.
16. Okun MS, Tagliati M, Pourfar M et al. Management of referred deep brain stimulation failures: a retrospective analysis from 2 movement disorders centers. *Arch Neurol* 2005;62:1250–1255.
17. van den Munckhof P, Contarino MF, Bour LJ, Speelman JD, de Bie RM, Schuurman PR. Postoperative curving and upward displacement of deep brain stimulation electrodes caused by brain shift. *Neurosurgery* 2010;67:49–53. discussion 53–54.
18. Contarino MF, Bot M, Speelman JD et al. Postoperative displacement of deep brain stimulation electrodes related to lead-anchoring technique. *Neurosurgery* 2013;73: 681–688. discussion 188.
19. Zylka W, Sabczynski J, Schmitz G. A Gaussian approach for the calculation of the accuracy of stereotactic frame systems. *Med Phys* 1999;26:381–391.
20. Fitzpatrick JM, Konrad PE, Nickele C, Cetinkaya E, Kao C. Accuracy of customized miniature stereotactic platforms. *Stereotact Funct Neurosurg* 2005;83:25–31.
21. Hamani C, Saint-Cyr JA, Fraser J, Kaplitt M, Lozano AM. The subthalamic nucleus in the context of movement disorders. *Brain* 2004;127:4–20.
22. Krack P, Fraix V, Mendes A, Benabid AL, Pollak P. Postoperative management of subthalamic nucleus stimulation for Parkinson's disease. *Mov Disord* 2002;17 (Suppl. 3): S188–S197.
23. Steigerwald F, Muller L, Johannes S, Matthies C, Volkmann J. Directional deep brain stimulation of the subthalamic nucleus: a pilot study using a novel neurostimulation device. *Mov Disord* 2016;31:1240–1243.
24. Barbe MT, Maarouf M, Alesch F, Timmermann L. Multiple source current steering–a novel deep brain stimulation concept for customized programming in a Parkinson's disease patient. *Parkinsonism Relat Disord* 2014;20:471–473.
25. Miocinovic S, Noecker AM, Maks CB, Butson CR, McIntyre CC. Cicerone: stereotactic neurophysiological recording and deep brain stimulation electrode placement software system. *Acta Neurochir Suppl* 2007;97:561–567.
26. Chaturvedi A, Butson CR, Lempka SF, Cooper SE, McIntyre CC. Patient-specific models of deep brain stimulation: influence of field model complexity on neural activation predictions. *Brain Stimul* 2010;3:65–67.
27. Astrom M, Lemaire JJ, Wardell K. Influence of heterogeneous and anisotropic tissue conductivity on electric field distribution in deep brain stimulation. *Med Biol Eng Comput* 2012;50:23–32.
28. Butson CR, McIntyre CC. Tissue and electrode capacitance reduce neural activation volumes during deep brain stimulation. *Clin Neurophysiol* 2005;116:2490–2500.
29. McIntyre CC, Mori S, Sherman DL, Thakor NV, Vitek JL. Electric field and stimulating influence generated by deep brain stimulation of the subthalamic nucleus. *Clin Neurophysiol* 2004;115:589–595.
30. Frankemolle AM, Wu J, Noecker AM et al. Reversing cognitive-motor impairments in Parkinson's disease patients using a computational modelling approach to deep brain stimulation programming. *Brain* 2010;133:746–761.
31. Teplitzky BA, Zitella LM, Xiao Y, Johnson MD. Model-based comparison of deep brain stimulation array functionality with varying number of radial electrodes and machine learning feature sets. *Front Comput Neurosci* 2016;10:58.
32. Alonso F, Latorre MA, Goransson N, Zsigmond P, Wardell K. Investigation into deep brain stimulation lead designs: a patient-specific simulation study. *Brain Sci* 2016;6: 1–16.
33. Buhlmann J, Hofmann L, Tass PA, Hauptmann C. Modeling of a segmented electrode for desynchronizing deep brain stimulation. *Front Neuroeng* 2011;4:15.
34. van Dijk KJ, Verhagen R, Chaturvedi A et al. A novel lead design enables selective deep brain stimulation of neural populations in the subthalamic region. *J Neural Eng* 2015;12:046003.
35. Chaturvedi A, Foutz TJ, McIntyre CC. Current steering to activate targeted neural pathways during deep brain stimulation of the subthalamic region. *Brain Stimul* 2012;5:369–377.
36. Butson CR, McIntyre CC. Current steering to control the volume of tissue activated during deep brain stimulation. *Brain Stimul* 2008;1:7–15.
37. Wakana S, Jiang H, Nagae-Poetscher LM, van Zijl PC, Mori S. Fiber tract-based atlas of human white matter anatomy. *Radiology* 2004;230:77–87.
38. Tuch DS, Wedeen VJ, Dale AM, George JS, Belliveau JW. Conductivity tensor mapping of the human brain using diffusion tensor MRI. *Proc Natl Acad Sci USA* 2001;98: 11697–11701.
39. Hines ML, Carnevale NT. The NEURON simulation environment. *Neural Comput* 1997;9:1179–1209.

40. Sato F, Parent M, Levesque M, Parent A. Axonal branching pattern of neurons of the subthalamic nucleus in primates. *J Comp Neurol* 2000;424:142–152.
41. McIntyre CC, Richardson AG, Grill WM. Modeling the excitability of mammalian nerve fibers: influence of afterpotentials on the recovery cycle. *J Neurophysiol* 2002; 87:995–1006.
42. Butson CR, Cooper SE, Henderson JM, McIntyre CC. Patient-specific analysis of the volume of tissue activated during deep brain stimulation. *Neuroimage* 2007;34:661–670.
43. Miocinovic S, Parent M, Butson CR et al. Computational analysis of subthalamic nucleus and lenticular fasciculus activation during therapeutic deep brain stimulation. *J Neurophysiol* 2006;96:1569–1580.
44. Waln O, Jimenez-Shahed J. Rechargeable deep brain stimulation implantable pulse generators in movement disorders: patient satisfaction and conversion parameters. *Neuromodulation* 2014;17:425–430; discussion 430.
45. Timmermann L, Schupbach M, Hertel F et al. A new rechargeable device for deep brain stimulation: a prospective patient satisfaction survey. *Eur Neurol* 2013;69:193–199.
46. Contarino MF, Bour LJ, Verhagen R et al. Directional steering: a novel approach to deep brain stimulation. *Neurology* 2014;83:1163–1169.
47. Pena E, Zhang S, Deyo S, Xiao Y, Johnson MD. Particle swarm optimization for programming deep brain stimulation arrays. *J Neural Eng* 2017;14:016014.

